

滨岸相沉积物粒度分布次总体 沉积意义挖掘

——以塔里木盆地哈得油田东河塘组为例

袁瑞¹⁾, 刘学¹⁾, 朱锐²⁾, 韩登林²⁾

1) 长江大学地球物理与石油资源学院, 武汉, 430100;

2) 长江大学地球科学学院, 武汉, 430100



内容提要:滨岸相是海洋与陆地过渡的沉积环境。频率曲线为多峰形态的滨岸相沉积物粒度分布记录了复杂的沉积动力机制。笔者等以塔里木盆地哈得油田石炭系东河塘组古代滨岸相砂体为例,挖掘滨岸相沉积物粒度分布次总体的沉积意义。利用偏正态概率密度函数从156份粒度分布数据中分离得到968个次总体,运用层次聚类分析次总体的类型,结合Pearson相关系数、沉积微相和概率累积曲线探讨次总体的关联性、组合模式、沉积环境意义和搬运方式。次总体可分为8种类型;粒度分布中随着细砂质主导次总体占比的增加,中砂质次总体占比随之增加、细砂—极细砂质次总体占比随之减少;坝体内中砂质次总体占比向上先增大后减小,滩体中极细砂—粉砂质次总体和粉砂质次总体含量明显增加,槽体内黏土质次总体占比一般大于6%;向海方向上,临滨坝、滩和槽内细砂质主导次总体峰值频率逐渐减小、分选性逐渐变差,粉砂质及黏土质组分逐渐增多;中砂质次总体的粗粒主要由上冲作用搬运,细砂质与细砂—极细砂质颗粒主要由回流作用搬运,粉砂质与黏土质颗粒分别沉积于递变悬浮和均匀悬浮过程中。基于粒度分布次总体的沉积信息挖掘可为现代和古代滨岸相沉积环境和沉积过程研究提供参考。

关键词:塔里木盆地;东河塘组;滨岸相;沉积物;粒度分布;次总体

沉积物是地球内外营力共同塑造地表形态的动态产物,可以系统揭示岩石圈、水圈、生物圈和大气圈等地球系统的演化历史、控制机制和相互作用(王成善等, 2025)。碎屑沉积物占地球表面约70%的面积,碎屑颗粒是风化剥蚀、搬运媒介和沉积环境等源—汇系统的经历者(Hartmann and Flemming, 2007; 蒋璟鑫等, 2020; Román-Sánchez et al., 2021; Yuan Rui et al., 2025a)。因此,由不同直径颗粒体积或重量百分比组成的碎屑沉积物粒度分布是原始沉积信息的载体(Bright et al., 2020; 袁瑞, 2025)。针对碎屑沉积物粒度分布的沉积解释甚至早于沉积学作为独立学科体系的构建(Sternberg, 1875; Udden, 1898, 1914; Wentworth, 1922; 王成善和林畅松, 2021; 王成善等, 2025)。为了解释粒度分布的沉积意义,早期形成了包括粒度分布参数统计(Krumbein and Pettijohn, 1938; Folk and Ward, 1957; Friedman, 1961)、Hjulstrom图解(Hjulstrom,

1936)、Sahu判别函数(Sahu, 1964)、C—M图版(Passega, 1964)、粒度指数(Doeglas, 1968)和概率累积曲线(Visher, 1969)等诸多方法,其中一些经典的研究手段至今仍被广泛使用。事实上,由不同水动力条件驱动的颗粒组分作为粒度分布的内部次总体,是碎屑沉积物的最小结构单元(Weltje and Prins, 2007; van Hateren et al., 2018)。复杂沉积过程下的沉积物由多个次总体叠加堆积而成,其粒度分布频率曲线呈现双峰或者多峰形态(Risovic, 1993; 孙东怀等, 2000; Xiao Jule et al., 2012; Wu Li et al., 2020; An Cheng et al., 2024; 袁瑞等, 2024)。基于统计学概率密度函数、采用曲线拟合技术分解粒度分布频率曲线,便可进一步提取得到单峰次总体(Ibbeken, 1983; Kondolf and Adhikari, 2000; Purkait, 2002; Sun Donghuai et al., 2004; 袁瑞等, 2022)。这些粒度分布次总体已为黄土、湖泊、河流和深海等多种沉积环境提供了更深层次的

注:本文为国家自然科学基金资助项目(编号:42202113)的成果。

收稿日期:2025-11-10;改回日期:2026-01-19;网络首发:2026-02-15;责任编辑:刘志强。Doi: 10.16509/j.georeview.2026.02.011

作者简介:袁瑞,男,1987年生,博士,副教授,硕士生导师,主要从事地球科学数据挖掘及测井地质方面的科研与教学工作;Email: yuanrui@yangtzeu.edu.cn。

沉积信息 (Carder et al., 1971; Ashley, 1978; Sun Donghuai et al., 2002; Gan and Scholz, 2017; 袁瑞, 2025)。

海岸带是海洋和陆地相互作用、相互影响的缓冲和过渡地带(庞文鸿, 2021)。海岸系统作为陆地物质输出与海洋泥沙输入的纽带,其沉积动力过程对全球海平面变化、岸线迁移、人类活动及资源利用具有深远影响(Newton and Icely, 2008; Ramesha et al., 2015; 骆永明, 2016; 郭兴杰等, 2025)。按照岸滩的组成物质,海岸可分为砂质海岸、基岩海岸、淤泥海岸、生物海岸和冰冻海岸等类型(索安宁等, 2015; 修淳等, 2022)。其中,被沿岸流、波浪及潮汐等多种沉积作用共同影响的砂质海岸为沿岸—离岸—离岸输沙过程提供主要场所,是海洋学和地质学研究的热点之一(姜在兴等, 2015; 尹力等, 2022; 潘毅等, 2024; 赵俊威等, 2025)。在沉积学中,一般将浪基面至海岸沙丘之间的砂质海岸沉积环境称为滨岸相(James and Dalrymple, 2010; 姜在兴和陈代钊, 2022)。由砂质、粉砂质及黏土质颗粒组成的滨岸相沉积物是研究现代和古代滨岸相沉积环境和水动力机制的基础数据。然而,滨岸相沉积物粒度分布频率曲线常为多峰形态,当前主要利用传统的统计参数、概率累积曲线和 C—M 图版等方法解释沉积意义,尚未见深入粒度分布次总体的相关报道 (Visher, 1969; 操应长等, 2010; 王萌等, 2020; 马彬彬等, 2022; Li Weilu et al., 2023; 黄继新等, 2025; 叶蓉等, 2025)。

塔里木盆地哈得油田石炭系东河塘组砂岩储层是我国首个发现的高产海相滨岸砂岩油藏(李维禄等, 2017)。笔者等以哈得油田东河塘组 6 口取心井 156 份古代滨岸相沉积物粒度分布数据为例,参考 Folk(1954)砂岩命名方案,识别滨岸相沉积物岩性;采用偏正态概率密度函数提取各个粒度分布中的次总体,计算次总体统计参数;利用层次聚类方法对次总体进行分类,揭示不同类型次总体参数特征;根据次总体占比特征解析次总体的关联性和组合模式;结合沉积微相,探讨地层纵向与横向粒度分布次总体变化规律;借助粒度分布概率累积曲线讨论次总体的搬运方式。笔者等旨在深入挖掘滨岸相沉积物粒度分布次总体蕴含的沉积属性,为现代和古代滨岸相沉积环境和沉积过程研究提供参考。

1 数据来源

1.1 地质概况

哈得油田位于新疆维吾尔自治区阿克苏地区沙雅县境内,构造位于塔里木盆地台盆区北部坳陷向塔北隆起的过渡部位(图 1a)(Zhao Jier et al., 2023)。哈得油田是我国探明的首个亿吨级沙漠整装油田,主力含油层系为石炭系东河塘组砂岩油藏(李维禄等, 2017)。东河塘组厚度为 0~40 m,埋深超 5000 m,其下伏为志留系泥岩,顶部在石炭系巴楚组沉积早期遭受剥蚀,并被角砾岩覆盖,最终形成“下超—顶剥”的地层模式(图 1b、c)(赵俊威等, 2018; Zhao Jier et al., 2023)。东河塘组砂岩为构造缓坡背景下无障壁浪控砂质滨岸碎屑沉积体,岩性以灰色、灰白色细粒砂岩为主,夹粉砂质及泥质砂岩(Li Weilu et al., 2023)。颗粒分选较好,磨圆度为中等—好,颗粒成分以石英为主,其次为岩屑和长石,成分成熟度和结构成熟度较高(赵俊威等, 2018)。受沉积与成岩作用影响,砂岩中钙质胶结物发育(赵俊威等, 2017; Yuan Rui et al., 2025b)。

1.2 基础资料

研究资料来源于哈得油田石炭系东河塘组 6 口重点取心井,岩心总长度为 61.42 m。塔里木油田公司共采集 156 份东河塘组岩石样本,参照石油天然气行业标准实施粒度分析测试(国家能源局, 2009)。测量得到粒度分布粒径范围为 0.98~1000 μm ($10\sim 0\ \phi$, $\phi = -\log_2 d$, d 为颗粒直径,单位 mm),粒级间隔为 0.25 ϕ (图 2)。采用 Folk-Ward 图解法计算粒度均值、方差、偏度和峰度(Folk and Ward, 1957)。收集裸眼井常规测井资料,其中自然伽马测井值(GR , API)能较好指示地层岩性:纯砂岩主要为低 GR 值;地层泥质含量较高时, GR 值偏高。将岩心岩性与粒度分析取样深度校正至井筒深度,形成 GR 测井曲线、钻井岩心和取样深度等单井综合资料(图 1c)。

2 研究方法

2.1 粒度分布分解

基于概率密度函数的粒度分布分解方法认为单一沉积动力所搬运的次总体服从某种统计分布(Kondolf and Adhikari, 2000; Purkait, 2002; Sun Donghuai et al., 2004; Wu Li et al., 2020; 袁瑞, 2025)。设东河塘组滨岸相沉积物粒度分布次总体服从偏正态概率分布,则粒度分布频率数据可视为若干个偏正态概率密度函数的线性组合(Gan and Scholz, 2017; 袁瑞等, 2022):

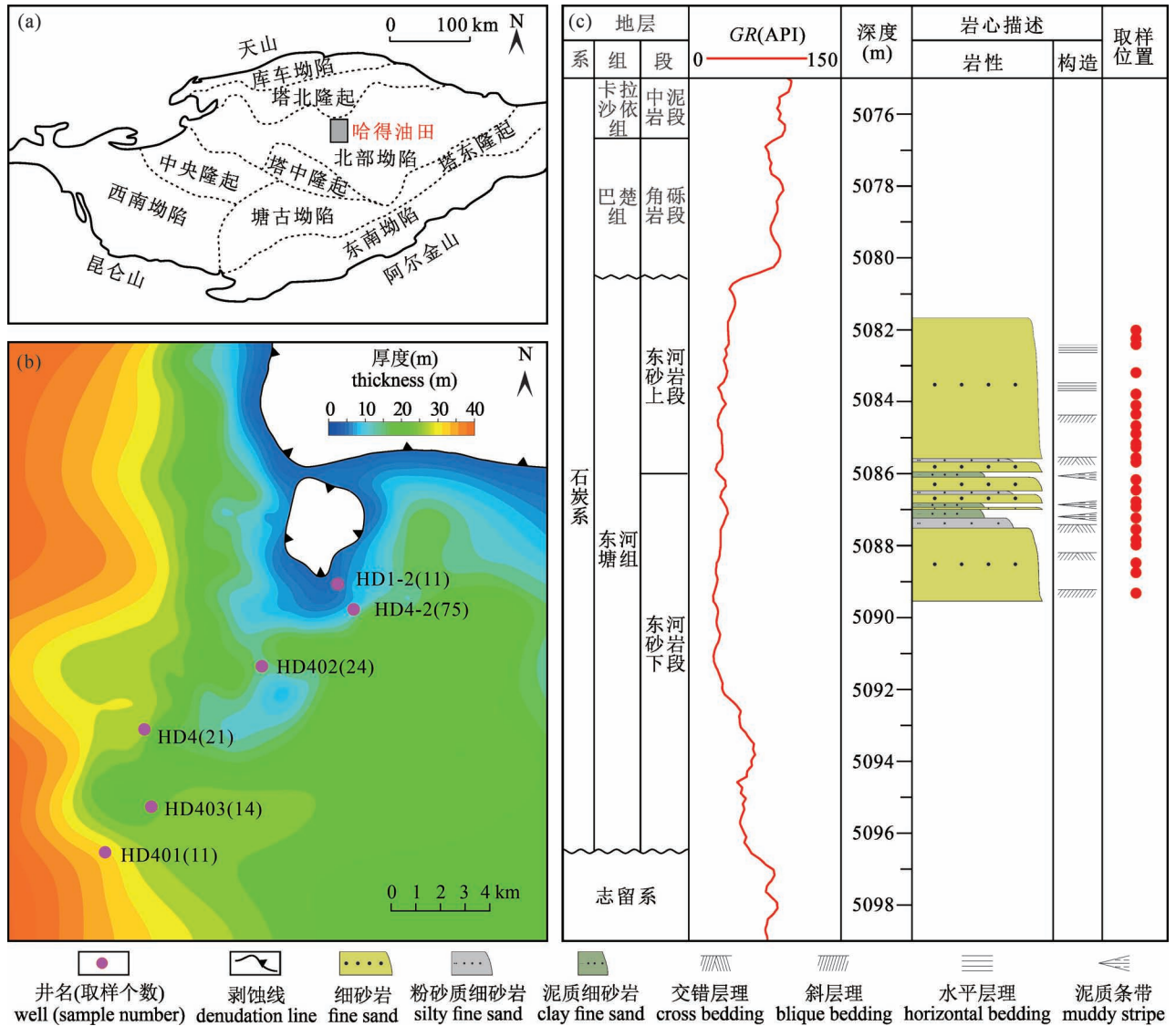


图1 哈得油田东河塘组地质背景及粒度分析取样井位

Fig. 1 Geological background of the Donghetang Formation in the Hade Oilfield and grain-size analysis samples in wells (a) 哈得油田构造位置; (b) 哈得油田东河塘组残余厚度平面图; (c) HD402 井 GR 测井曲线、岩心描述和粒度分析取样位置综合柱状图
 (a) tectonic location of the Hade Oilfield in the Tarim Basin; (b) residual thickness distribution of the Donghetang Formation in the Hade Oilfield; (c) composite chart of the GR logging curve, coring description and sampling location of grain-size analysis in the Well HD402

$$f(y) = \sum_{i=1}^n c_i \left\{ \frac{1}{\pi\sigma_i} \exp\left(-\frac{(x-\mu_i)^2}{2\sigma_i^2}\right) \int_{-\infty}^{\frac{x-\mu_i}{\sigma_i}} \exp\left(-\frac{t^2}{2}\right) dt \right\} \quad (1)$$

其中 $f(y)$ 为粒度分布的拟合值; x 为粒度分布粒级; ϕ ; c_i 为第 i 个次总体在粒度分布中的占比, $\sum c_i = 100\%$; μ_i 为第 i 个次总体偏正态分布的位置参数; σ_i 为第 i 个次总体偏正态分布的尺度参数, α_i 为第 i 个次总体偏正态分布的形状参数。根据以上次总体参数, 可进一步计算次总体的峰值频率、均值、方差、偏度和峰度等统计参数 (Gan and Scholz, 2017;

袁瑞等, 2022)。同时, 利用粒度分布拟合值与实验值的均方根误差评价粒度分布次总体分离效果。

2.2 聚类分析

聚类分析将数据样本按照不同的属性特征进行自动分类, 是一种无监督机器学习 (Bergen et al., 2019)。层次聚类分析采用“自下而上”的凝聚或者“自上而下”的分裂方法, 按照样本之间的距离连接得到树状图, 是无预先定义类别中常用分类方法之一 (林情闽, 2023)。其中凝聚式层次聚类首先把每个样本点当成一个集合, 计算集合之间的两两距离; 其次根据特定连接方式找出距离最小的两个集合,

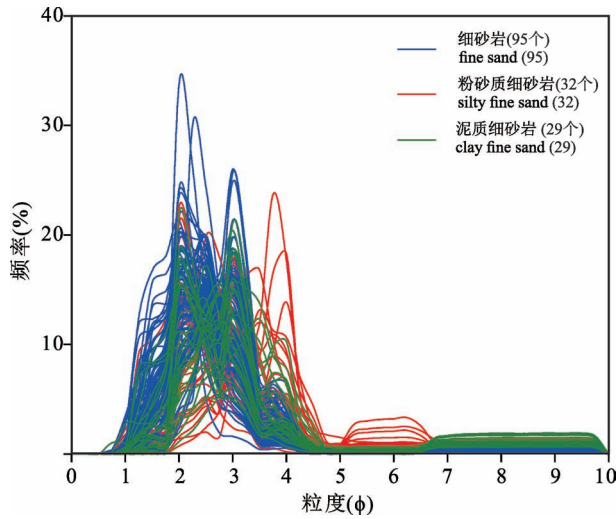


图2 哈得油田东河塘组滨岸相 156 份沉积物粒度分布频率曲线

Fig. 2 Grain-size distribution frequency curves of 156 littoral facies sediments from the Donghetang Formation in the Hade Oilfield

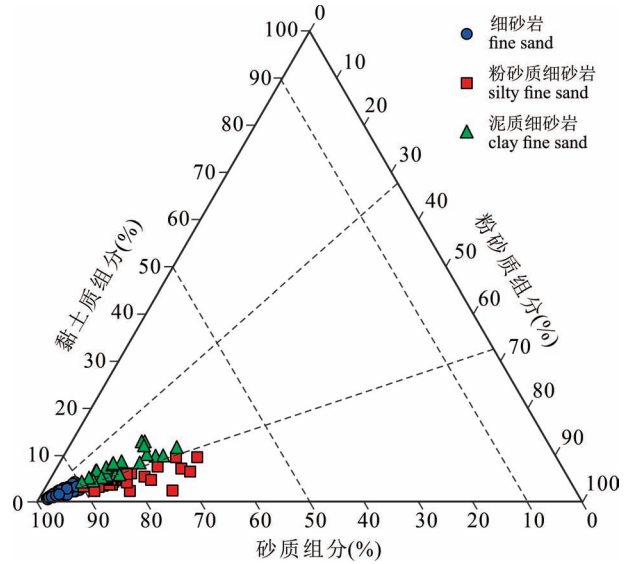


图3 哈得油田东河塘组滨岸相沉积物岩性分类三角图
Fig. 3 Ternary plot of lithological classification for littoral facies sediments from the Donghetang Formation in the Hade Oilfield

合并为新集合,重新计算集合之间的距离,如此循环,直至一个集合;然后根据集合合并的先后顺序画出树状图;最终选取合适的群组分类(余恒和侯晓岚, 2022)。笔者等选用欧几里得距离度量粒度分布次总体样本之间的距离:

$$d_{i,j} = \left[\sum_{k=1}^n (x_{i,k} - x_{j,k})^2 \right]^{\frac{1}{2}} \quad (2)$$

其中 $x_{i,k}$ 与 $x_{j,k}$ 分别为第 i 个与 j 个粒度分布次总体集合的第 k 个粒级对应的频率数据。

3 结果

3.1 粒度分布特征

在哈得油田东河塘组浪控滨岸相环境中(李维禄等, 2017; 赵俊威等, 2018; Li Weilu et al., 2023; Zhao Jier et al., 2023; Yuan Rui et al., 2025b),沉积物粒度分布频率曲线均为多峰形态(图2)。参照 Wentworth(1922)碎屑沉积物粒级划分标准,峰值粒径主要位于 $1.5 \sim 3.5 \phi$,对应细砂和极细砂,粉砂质颗粒含量小于 25%,黏土质颗粒含量小于 15%,少中砂,不含粗砂(图2)。利用 Folk(1954)碎屑沉积物砂—粉砂—黏土组分三端元定名方案可知(Blott and Pye, 2012),东河塘组滨岸相沉积物样品包括 95 份细砂岩、32 份粉砂质细砂岩和 29 份泥质细砂岩(图3)。细砂岩的粒度均值为 $2 \sim 3 \phi$,方差为 $0.5 \sim 1.5$,对应分选性中等—差,以细

偏为主、极细偏次之,峰度分布范围较大。粉砂质细砂岩和泥质细砂岩的粒度均值($2.5 \sim 4.5 \phi$)、方差($1.3 \sim 2.7$)、偏度($0.3 \sim 0.8$)和峰度($1.6 \sim 3.0$)分布范围相近。

3.2 次总体分离

利用偏正态概率密度函数逐个从东河塘组沉积物粒度分布中分离提取次总体,计算每个次总体峰值频率、在粒度分布中占比、均值、方差、偏度及峰度等参数。例如,HD4 井 5075.45 m 处粉砂质细砂岩粒度分布频率曲线为明显多峰形态,其均值为 3.1ϕ ,砂质、粉砂质和黏土质组分含量分别为 82.3%、12.2%和 5.5%。从该粒度分布中共分离 8 个次总体,次总体波峰与粒度分布频率曲线波峰具有较好的对应关系(图4)。均值为 2.2ϕ 的次总体峰值频率(19.4%)和占比(46.5%)最大,是沉积物的主要颗粒组分。均值为 2.9ϕ 的次总体峰值频率和占比分别为 8.8%和 24.6%,是粒度分布的次要颗粒组分。均值为 7.0ϕ 的次总体尽管峰值频率仅为 1.1%,但是其方差大(2.1)、分选性差,在粒度分布中占比达 13.2%,与沉积物中粉砂质含量接近。均值为 9.2ϕ 的次总体是沉积物中最细组分,在粒度分布中占比为 4.4%,主要对应黏土质组分。其他次总体均值均小于 4ϕ ,峰值频率均小于 4%,在粒度分布中占比均小于 7%,分选性好。该 8 个次总体之和即为粒度分布的拟合值,其与粒度分布实验值

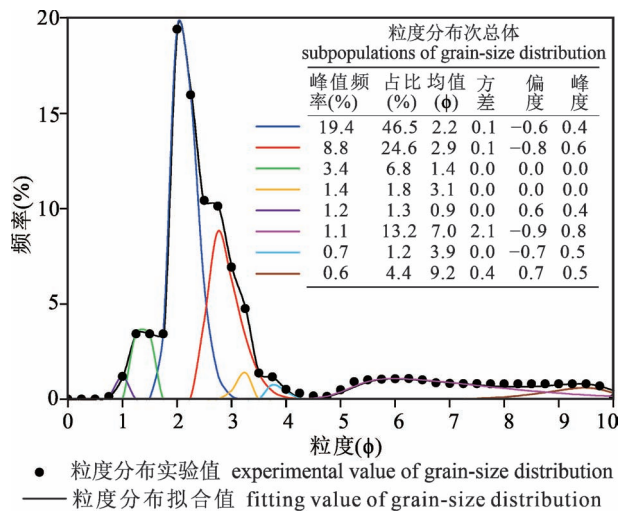


图4 哈得油田 HD4 井 5075.45 m 粉砂质细砂岩
粒度分布的次总体分离结果

Fig. 4 Subpopulation decomposed results of silty fine sand in 5075.45 m of Well HD4 in the Hade Oilfield

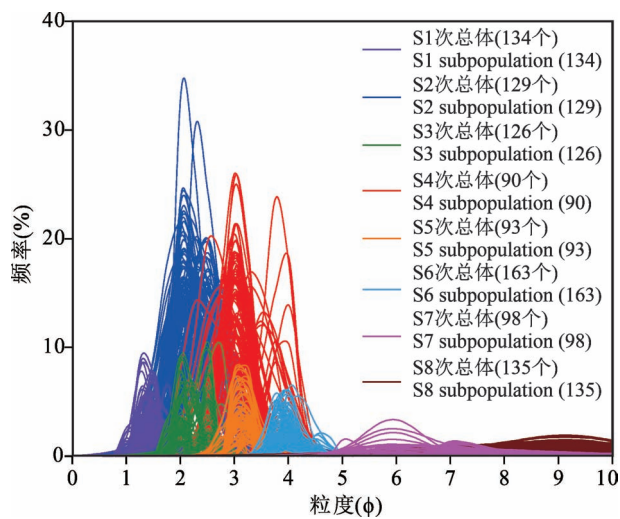


图5 哈得油田东河塘组滨岸相沉积物
粒度分布 968 个次总体

Fig. 5 All 968 subpopulations in grain-size distributions of littoral facies sediments from the Donghetang Formation in the Hade Oilfield

的均方根误差为 0.12%。最终,从哈得油田东河塘组沉积物每个粒度分布中分解得到 4~9 个次总体,共计 968 个(图 5),并计算每个次总体的统计参数。所有粒度分布拟合值与实验值的均方根误差均小于 0.75%,粒度分布次总体分离误差小。

3.3 次总体类型

为了明确东河塘组滨岸相砂岩粒度分布次总体

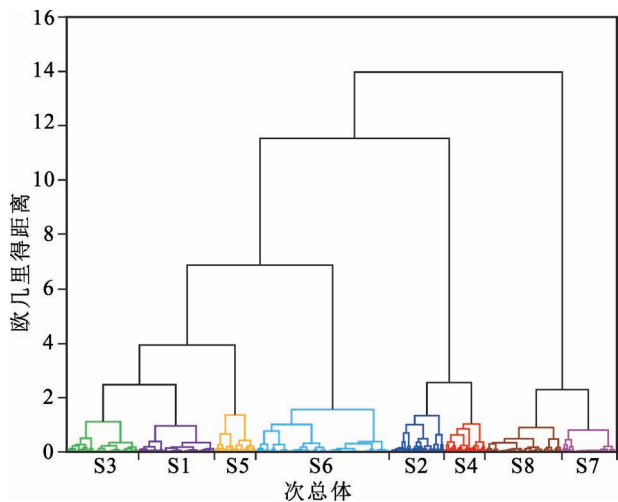


图6 哈得油田东河塘组滨岸相沉积物
粒度分布次总体层次聚类结果

Fig. 6 Hierarchical clustering result of subpopulations in grain-size distributions of littoral facies sediments from the Donghetang Formation in the Hade Oilfield

的类型,优选次总体峰值频率、占比和均值进行归一化处理,消除不同参数之间的量纲。采用凝聚式和欧几里得距离对次总体进行层次聚类分析。根据聚类分析结果树状图,综合考虑粒度分布次总体均值、峰值频率及占比特征,将次总体分为 8 种类型,分别命名为 S1~S8,并适当整理类别边界附近的次总体(图 6)。最终建立包含多种统计参数及类型的哈得油田东河塘组滨岸相沉积物粒度分布次总体数据集(图 5)。

图 7 展示了不同类型次总体峰值频率、在粒度分布中占比、均值、方差、偏度与峰度等参数特征。S1 次总体共 134 个,峰值频率小于 9%,在粒度分布中占比一般小于 15%,均值为 0.9~1.7 ϕ ,方差小于 0.2,代表中砂质组分,为滨岸相沉积物中相对较粗的颗粒(图 7a—c)。S2 次总体共 129 个,峰值频率为 7%~33%,在粒度分布中占比为 20%~85%,均值主要为 1.9~2.5 ϕ ,方差小于 0.5,对应细砂质组分,是沉积物中主导次总体之一(图 7a—c)。S3 次总体共 126 个,峰值频率小于 10%,在粒度分布中占比小于 18%,均值主要为 1.8~2.7 ϕ ,方差小于 0.3;尽管 S3 次总体也对应细砂质组分,但是其在沉积物中占比小于 S2 次总体(图 7a—c)。S4 次总体共 90 个,峰值频率为 8%~25%,在粒度分布中占比为 20%~72%,均值主要为 2.6~3.7 ϕ ,方差小于 0.3,主要涵盖细砂—极细砂质颗粒,是沉积物中另

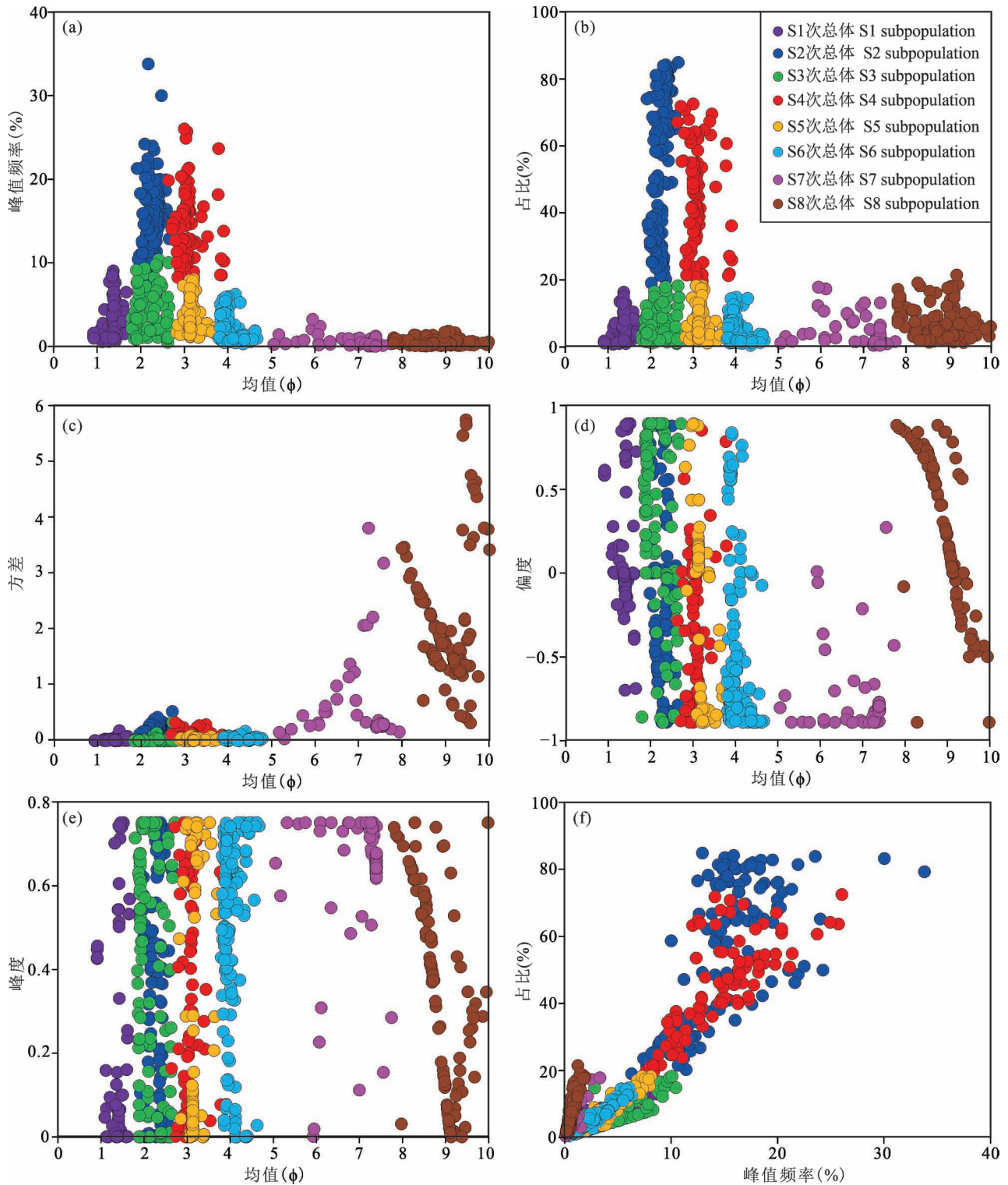


图7 哈得油田东河塘组滨岸相沉积物粒度分布不同类型次总体参数特征

Fig. 7 Parameter characteristics of different types of subpopulations in grain-size distributions of littoral facies sediments from the Donghetang Formation in the Hade Oilfield

(a) 次总体均值与峰值频率交会图; (b) 次总体均值与占比交会图; (c) 次总体均值与方差交会图; (d) 次总体均值与偏度交会图; (e) 次总体均值与峰度交会图; (f) 次总体峰值频率与占比交会图

(a) means and peak frequencies crossplot of subpopulations; (b) means and percentages crossplot of subpopulations; (c) means and sorting crossplot of subpopulations; (d) means and skewness crossplot of subpopulations; (e) means and kurtosis crossplot of subpopulations; (f) peak frequencies and percentages crossplot of subpopulations

一个主导次总体(图7a—c)。S5次总体共93个,峰值频率小于8%,在粒度分布中占比小于18%,均值主要为2.9~3.7 ϕ ,方差小于0.1;S5次总体也主要对应细砂—极细砂质颗粒,但是其在沉积物中占比小于S4次总体(图7a—c)。S6次总体共163个,峰值频率小于6%,在粒度分布中占比小于14%,均值主要为3.8~4.7 ϕ ,方差小于0.2,包括极细砂—粉砂质组分(图7a—c)。S7次总体共98个,峰值频率小于3%,在粒度分布中占比小于18%,均值为5.2~7.7 ϕ ,方差差异大(0.1~3.8),主要对应粉砂质颗粒(图7a—c)。S8次总体共135个,峰值频率小于2%,在粒度分布中占比小于20%,均值为7.8~10 ϕ ,方差分布范围大(0.3~5.7),主要包含黏土质组分,代表了沉积物中最细粒物质(图7a—c)。

综上所述,S1、S2、S3、S4、S5和S6次总体分选好,其中S2或S4次总体是沉积物的主导组分,S2与S3、S4与S5次总体分别具有相似的粒径分布区间。尽管S7和S8次总体的峰值频率均较小,但是部分次总体方差大,粒径分布范围大,在沉积物中占比仍然可达20%(图7a—c)。各种类型次总体偏度和峰度分布差异较大,没有明显集中范围(图7d—e)。S2和S4次总体峰值频率与占比呈较弱的线性正相关,S1、S3、S5、S6、S7和S8次总体峰值频率与占比呈较强线性正相关(图7f)。从而,在粒度分布多峰频率曲线中,根据较小波峰的频率值,选取对应次总体类型的峰值频率与占比经验公式,可以快速预测该波峰对应次总体在粒度分布中所占的比例。哈得油田东河塘组滨岸相沉积物粒度分布各类型次总体的参数特征见表1。

4 讨论

4.1 次总体关联性

在哈得油田东河塘组滨岸相沉积物粒度分布次

总体数据集中,利用Pearson相关系数分别评价细砂岩、粉砂质细砂岩和泥质细砂岩中8种次总体类型占比的关联性(图8)。Pearson系数介于-1与1之间,当Pearson系数大于0时,说明2类次总体为正相关,反之为负相关。在所有沉积物粒度分布中,S1与S2次总体均为中等正相关,指示随着中砂质组分的增加,占主导的细砂质组分相应增加。S2与S3次总体、S4与S5次总体均为中等负相关,这是因为S2与S3次总体、S4与S5次总体分别具有重合的粒径区间,在粒度分布中为互斥关系。3种岩性的S2与S4次总体之间Pearson系数均小于-0.85,为强负相关性,说明在各自粒度分布中占主导的S2与S4次总体“此消彼长”。从细砂岩至泥质细砂岩,S1与S4次总体的负相关性逐渐增强,指示随着细粒组分增加,占主导的细砂—极细砂质组分与中砂质组分的互斥性越强。

另外,在细砂岩中,S2与S5次总体、S4与S6次总体均为中等正相关,这是由于S2与S5次总体、S4与S6次总体的粒径区间是相邻的(图8a)。在粉砂质细砂岩中,S1与S8次总体、S2与S8次总体、S7与S8次总体均为中等负相关,暗示粉砂质细砂岩沉积物中砂质、细砂质和粉砂质组分越多,黏土质组分越少(图8b)。在泥质细砂岩中,S3与S1次总体、S3与S4次总体分别为中等负相关和中等正相关,说明含量较少的细砂质组分与中砂质组分是互斥的、与占主导极细砂质组分是相容的;粉砂质组分与黏土质组分相关性较弱(图8c)。

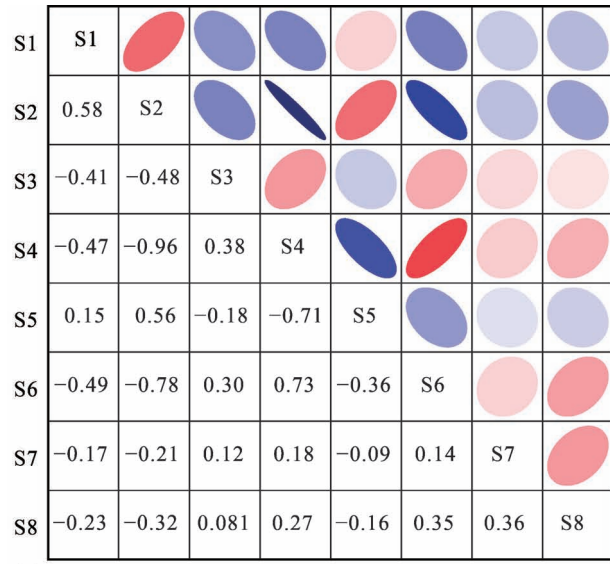
4.2 次总体组合模式

在东河塘组滨岸相沉积物中,根据粒度分布中S2与S4次总体的占比差异,可将粒度分布分为两种类型:①S2主导型,粒度分布中S2次总体为主,S4次总体占比小或无;②S4主导型,粒度分布中S4

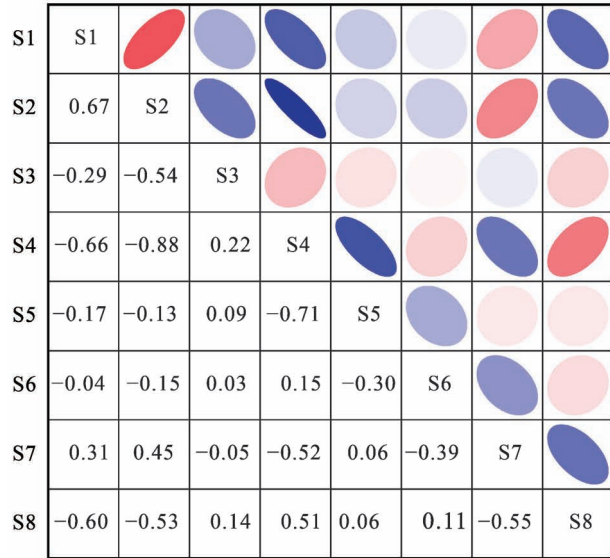
表1 哈得油田东河塘组滨岸相沉积物粒度分布次总体类型及其参数

Table 1 Types and parameters of subpopulations in grain-size distributions of littoral facies sediments from the Donghetang Formation in the Hade Oilfield

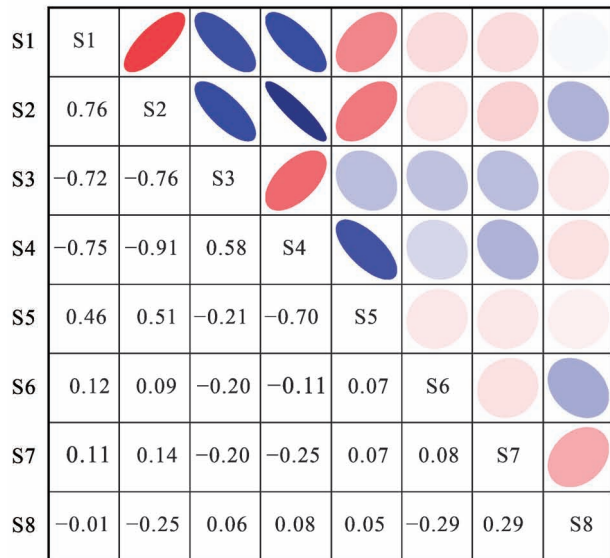
次总体类型	最大频率(%)	占比(%)	均值(ϕ)	方差	占比(y)与峰值频率关系(x)	粒度组分
S1	<9	<15	0.9~1.7	<0.2	$y = 1.5866x + 0.2107; R^2 = 0.8451$	中砂质组分,分选性极好
S2	7~33	20~85	1.9~2.5	<0.5	$y = 3.1298x + 8.1118; R^2 = 0.4163$	细砂质组分,分选性极好—好
S3	<10	<18	1.8~2.7	<0.3	$y = 1.4895x - 0.0232; R^2 = 0.7134$	细砂质组分,分选性极好
S4	8~25	20~72	2.6~3.7	<0.3	$y = 2.6291x + 6.5345; R^2 = 0.5764$	细砂—极细砂质组分,分选性极好
S5	<8	<18	2.9~3.7	<0.1	$y = 2.2327x - 0.7325; R^2 = 0.9042$	细砂—极细砂质组分,分选性极好
S6	<6	<14	3.8~4.7	<0.2	$y = 2.185x - 0.1437; R^2 = 0.9371$	极细砂—粉砂质组分,分选性极好
S7	<3	<18	5.2~7.7	0.1~3.8	$y = 6.2493x - 0.057; R^2 = 0.7691$	粉砂质组分,分选性差异大
S8	<2	<20	7.8~10	0.3~5.7	$y = 11.676x + 0.0234; R^2 = 0.8317$	黏土质组分,分选性差异大



(a) S1 S2 S3 S4 S5 S6 S7 S8



(b) S1 S2 S3 S4 S5 S6 S7 S8



(c) S1 S2 S3 S4 S5 S6 S7 S8

次总体为主, S2次总体占比相对小或无。为了解析滨岸相沉积物中不同粒度组分次总体的组合模式, 统计分析不同岩性、不同类型粒度分布次总体占比的最小值、最大值和平均值(表2)。细砂岩粒度分布以 S2 主导型为主, S4 主导型次之; 粉砂质细砂岩和泥质细砂岩粒度分布以 S4 主导型为主, S2 主导型次之。细砂岩粒度分布 S2 主导型主要由 S2、S5、S1 次总体组成, S4 主导型主要由 S4、S2、S6 和 S3 次总体组成。粉砂质细砂岩粒度分布 S2 主导型主要由 S2、S4、S7、S8 和 S1 次总体组成, S4 主导型主要由 S4、S8、S2、S3 和 S6 次总体组成。泥质细砂岩粒度分布 S2 主导型主要由 S2、S8、S4、S5 和 S1 组成, S4 主导型主要由 S4、S8、S2、S3 和 S6 次总体组成。S2 主导型粒度分布中, 从细砂岩到泥质细砂岩, 代表黏土质组分的 S8 次总体占比逐渐增大, 对应中砂质组分的 S1 次总体占比逐渐减小。S4 主导型粒度分布中, 代表中砂质组分的 S1 次总体整体不发育; 对应极细砂—粉砂质组分的 S6 次总体较发育; 从细砂岩到泥质细砂岩, S4 次总体占比平均值逐渐增大。

4.3 次总体沉积环境意义

据前人研究结果, 整个塔北地区石炭系东河塘组是晚志留世至早石炭世海侵背景下的滨岸相砂岩沉积体, 哈得油田处于该沉积体系的靠岸末缘(王涛等, 2018; Li Weilu et al., 2023)。完整的滨岸相沉积环境一般包括岸后沙丘、后滨、前滨、临滨 4 种亚相(Visher, 1969; Komar, 1997; 王萌等, 2020; 赵俊威等, 2025)。但是在哈得油田东河塘组岩心观察和薄片资料中并未发现岸后沙丘和后滨中典型的石英毛玻璃和生物介壳特征, 因此认为该地层主要发育前滨和临滨两种沉积亚相(赵俊威等, 2017, 2018)。前滨位于海滩下部平均高潮线和平均低潮线之间, 临滨是平均低潮线与正常浪基面之间的地区(Komar, 1997; James and Dalrymple, 2010; 王萌等, 2020)。在层序地层中, 哈得油田东河塘组由下

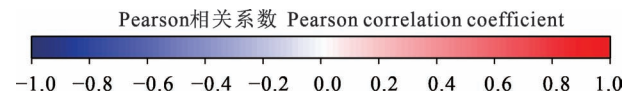


图 8 哈得油田东河塘组滨岸相不同岩性沉积物粒度分布次总体相关性

Fig. 8 Correlations of subpopulations in grain-size distributions of littoral facies different lithological sediments from the Donghetang Formation in the Hade Oilfield

(a) 细砂岩; (b) 粉砂质细砂岩; (c) 泥质细砂岩

(a) fine sands; (b) silty fine sands; (c) muddy fine sands

表 2 哈得油田东河塘组滨岸相不同类型沉积物粒度分布的次总体占比统计及组合

Table 2 Percentage statistics and combinations of subpopulations in different types of grain-size distributions of littoral facies from the Donghetang Formation in the Hade Oilfield

岩性	粒度分布类型	次总体在粒度分布中占比(%)								主要组成次总体
		S1	S2	S3	S4	S5	S6	S7	S8	
细砂岩	S2 主导型 (68 个)	$\frac{0 \sim 16.3}{6.2}$	$\frac{36.8 \sim 84.9}{73.2}$	$\frac{0 \sim 14.8}{2.9}$	$\frac{0 \sim 32.0}{2.4}$	$\frac{0 \sim 18.3}{7.1}$	$\frac{0 \sim 8.7}{2.5}$	$\frac{0 \sim 2.1}{0.4}$	$\frac{0 \sim 8.0}{2.5}$	S2, S5, S1
	S4 主导型 (27 个)	$\frac{0 \sim 6.5}{2.1}$	$\frac{0 \sim 38.7}{26.8}$	$\frac{0 \sim 17.9}{5.9}$	$\frac{36.5 \sim 72.5}{50.7}$	$\frac{0 \sim 0}{0}$	$\frac{3.2 \sim 11.7}{6.8}$	$\frac{0 \sim 5.3}{0.8}$	$\frac{0 \sim 7.3}{3.6}$	S4, S2, S6, S3
粉砂质细砂岩	S2 主导型 (11 个)	$\frac{1.9 \sim 15.0}{6.1}$	$\frac{31.6 \sim 63.6}{45.9}$	$\frac{0 \sim 18.3}{3.0}$	$\frac{0 \sim 35.8}{20.7}$	$\frac{0 \sim 7.1}{2.8}$	$\frac{0 \sim 10}{2.8}$	$\frac{0 \sim 17.8}{9.1}$	$\frac{2.6 \sim 11.9}{6.2}$	S2, S4, S7, S8, S1
	S4 主导型 (21 个)	$\frac{0 \sim 13.0}{2.7}$	$\frac{0 \sim 34.0}{9.1}$	$\frac{0 \sim 16.6}{7.7}$	$\frac{35.4 \sim 71.8}{54.0}$	$\frac{0 \sim 14.6}{2.9}$	$\frac{0 \sim 14.8}{7.1}$	$\frac{0 \sim 13.2}{3.9}$	$\frac{2.3 \sim 18.2}{9.5}$	S4, S8, S2, S3, S6
泥质细砂岩	S2 主导型 (13 个)	$\frac{1.1 \sim 9.5}{5.6}$	$\frac{34.9 \sim 65.3}{50.9}$	$\frac{0 \sim 8.6}{1.5}$	$\frac{0 \sim 37.0}{12.6}$	$\frac{0 \sim 18.2}{6.8}$	$\frac{0 \sim 7.4}{4.1}$	$\frac{0 \sim 6.5}{2.8}$	$\frac{9.5 \sim 18.1}{13.1}$	S2, S8, S4, S5, S1
	S4 主导型 (16 个)	$\frac{0 \sim 8.1}{1.8}$	$\frac{0 \sim 25.4}{10.3}$	$\frac{0 \sim 13.7}{7.0}$	$\frac{41.4 \sim 70.8}{55.8}$	$\frac{0 \sim 7.7}{1.1}$	$\frac{0 \sim 12.6}{6.5}$	$\frac{0 \sim 5.0}{2.1}$	$\frac{7.0 \sim 21.5}{13.1}$	S4, S8, S2, S3, S6

注: $\frac{0 \sim 16.3}{6.2}$ 为 $\frac{\text{最小值} - \text{最大值}}{\text{平均值}}$

段退积式和上段进积式两种沉积序列组成;退积式沉积序列自下而上发育前滨—临滨亚相;进积式沉积序列自下而上发育临滨—前滨亚相,但其前滨亚相在巴楚组沉积早期多被暴露剥蚀(赵俊威等, 2017, 2018)(图 9)。

根据滨岸相古地貌形态,前滨和临滨亚相可分别划分为坝、滩、槽 3 种沉积微相(姜在兴等, 2015; 赵俊威等, 2024)。坝体平面呈长条形或长椭圆形,垂向呈底平顶凸形态。滩为波浪双向水流冲刷下相对平坦区域。槽为坝后凹槽位置,平面一般为长椭圆形或新月形,垂向呈底凹顶平形态(王涛等, 2018)。通过岩心观察,认为哈得油田东河塘组滨岸相前滨坝和临滨坝多发育块状层理、平行层理、低角度交错层理和斜层理细砂岩。前滨滩和临滨滩多发育平行层理和低角度交错层理粉砂质细砂岩,近陆区沉积厚度小。坝后凹槽水体能量相对较弱,多发育泥质条带和平行层理泥质细砂岩(图 10)。

前滨坝、滩、槽和临滨坝、滩、槽微相沉积物均可分为 S2 或 S4 主导型粒度分布。垂向上,在前滨坝与临滨坝内对应中砂质组分的 S1 次总体占比由下至上先增大后减小,暗示波浪控制下的沉积动力微尺度周期性变化:波浪能量较弱时,以 S2 与 S4 次总体为主的细砂和极细砂质颗粒堆积;波浪能量较强时,中砂质组分被带入。另外,前滨坝与临滨坝中 S7 与 S8 次总体含量较少,说明粉砂质和黏土质组分不发育。前滨滩与临滨滩沉积物中 S6 次总体占比一般大

于 8%、S7 次总体含量般大于 4%,说明极细砂和粉砂质组分较发育。前滨槽与临滨槽沉积物中 S8 次总体一般大于 6%,说明黏土质组分含量较多(图 9)。

在上段进积式沉积序列中,从临滨坝至临滨滩和临滨槽,沉积物粒度分布 S2 次总体峰值频率逐渐减小、分选性逐渐变差,S6、S7、S8 次总体占比逐渐增大。向海方向上,临滨坝、滩、槽内沉积物粒度分布 S7、S8 次总体含量分别逐渐增多,并且临滨槽内占主导的 S2 或者 S4 次总体峰值频率及占比逐渐减小。说明在水体变深、水动力减弱的沉积环境变化趋势下,滨岸相沉积物细砂质组分逐渐减少,细粒组分逐渐增多(图 11)。需要指出的是,东河塘组残余厚度小、沉积动力突变小,前滨与临滨两种沉积亚相整体粒度组分差异不大,难以仅利用粒度分布次总体区分沉积亚相。

4.4 次总体搬运方式

浪控作用下的滨岸相是砂质海岸带中泥沙运动最剧烈的区域之一,前滨和临滨微相中向岸—离岸输沙过程主要是在冲流带中完成的,冲流过程包括水体向陆上冲和向海回流两种沉积作用(Masselink and Puleo, 2006; 姜在兴等, 2015; Jackson et al., 2017; 潘毅等, 2024; 尹力等, 2024)。众多文献中古代和现代滨岸相沉积物粒度分布的概率累积曲线多为双跳跃组分特征(Visher, 1969; 王萌等, 2020; 黄继新等, 2025; 叶蓉等, 2025)。哈得油田东河塘组滨岸相 S2 或者 S4 主导型细砂岩、粉砂质细砂岩

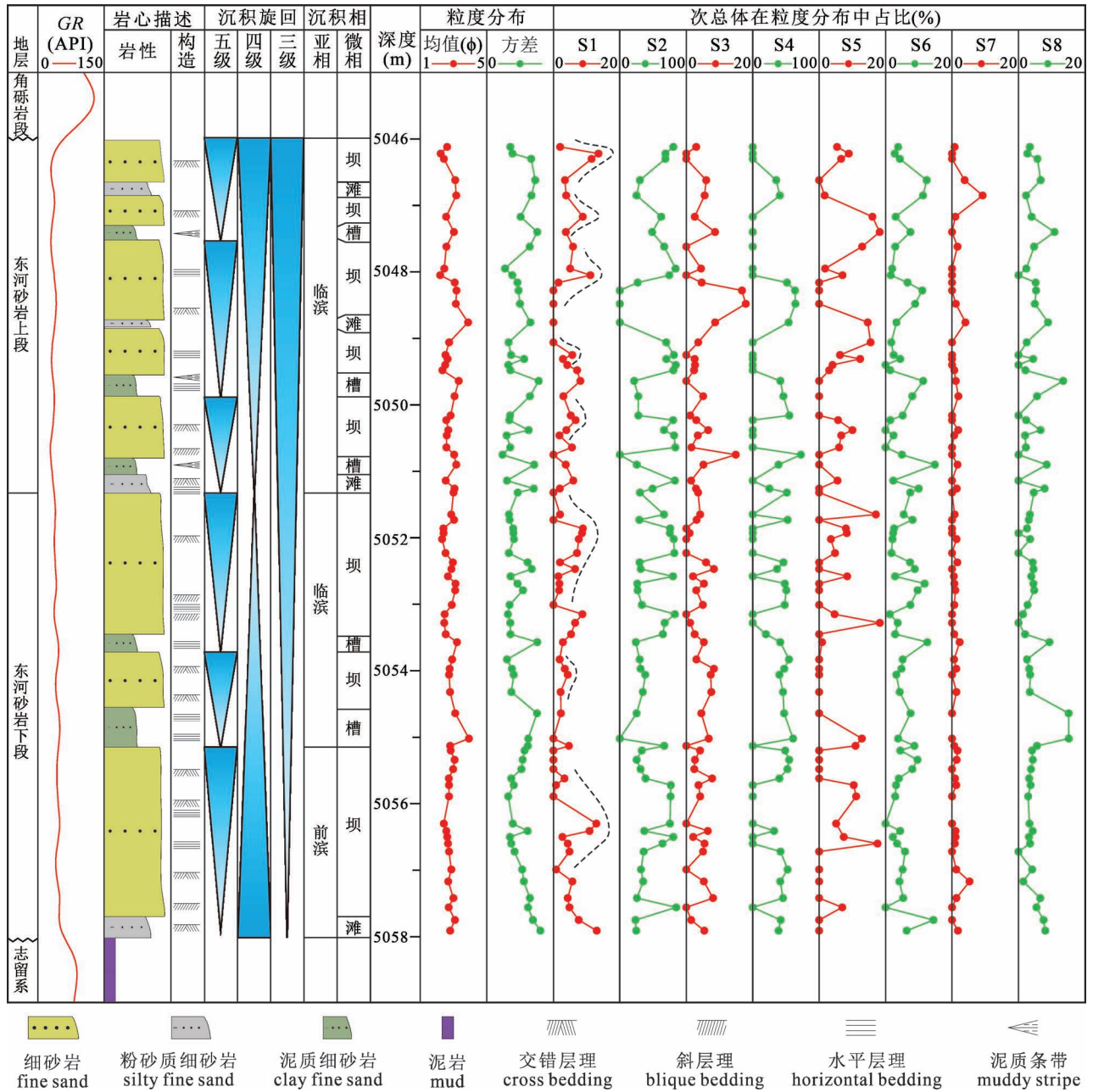


图9 哈得油田 HD4-2 井东河塘组测井、岩心、层序、沉积及次总体参数综合柱状图

Fig. 9 Composite chart of log, core, sequence, sedimentary and subpopulation parameters in the Well HD4-2 in the Hade Oilfield

及泥质细砂岩粒度分布概率累积曲线均具有以下2个显著特征:①概率累积曲线主要分为跳跃与悬浮2段式,无滚动组分。跳跃段又可分为2部分,两者的斜率稍有差别,分别指示冲流带上冲和回流两种沉积过程(Visher, 1969; 马彬彬, 2022; 潘毅等, 2024; 黄继新等, 2025; 叶蓉等, 2025)。悬浮段亦可分为2部分,两者在粒径区间跨度和斜率差异较大,分别对应递变悬浮与均匀悬浮沉积(Passega, 1964)。②跳跃组分与悬浮组分的粒径截断点在

3.5 ϕ 附近,上冲和回流粒径截断点一般位于1.5 ϕ 附近,递变悬浮与均匀悬浮粒径截断点主要在8 ϕ 附近。对照粒度分布次总体的粒径区间,推断上冲作用主要搬运S1次总体的粗粒组分;回流作用主要搬运S2、S3、S4及S5等细砂质和极细砂质次总体,是哈得油田东河塘组滨岸相沉积物的主要搬运方式;对应极细砂—粉砂质组分的S6次总体为跳跃向悬浮搬运的过渡组分;S7次总体与部分S8次总体对应的粉砂质颗粒主要依靠递变悬浮作用沉淀;S8



图 10 哈得油田东河塘组滨岸相典型岩性及沉积构造

Fig. 10 Typical lithology and sedimentary structure of littoral facies from the Donghetang Formation in the Hade Oilfield

次总体与部分 S7 次总体对应的黏土质颗粒主要依靠均匀悬浮作用缓慢堆积(图 12)。因此,分离得到粒度分布次总体后,可明确滨岸相沉积物颗粒的搬运方式。

5 结论

以塔里木盆地哈得油田石炭系东河塘组 6 口取心中 156 份粒度分布数据为例,挖掘古代滨岸相沉积物粒度分布次总体的沉积意义,得到以下结论和认识:

(1) 哈得油田东河塘组滨岸相主要发育细砂岩、粉砂质细砂岩和泥质细砂岩。利用偏正态概率密度函数从粒度分布数据中共分离得到 968 个次总体。采用层次聚类分析方法将次总体分为 8 种类型:中砂质次总体、主导细砂质次总体、占比较少细

砂质次总体、主导细砂—极细砂质次总体、占比较少细砂—极细砂质次总体、极细砂—粉砂质次总体、粉砂质次总体和黏土质次总体。

(2) 所有沉积物中至少包含 1 个主导细砂质次总体或主导细砂—极细砂质次总体。随着主导细砂质次总体占比的增加,中砂质次总体占比随之增加、主导细砂—极细砂质次总体占比随之减少。在细砂岩中,粒径区间相邻的砂质次总体均为中等正相关。在粉砂质细砂岩中,中砂质、细砂质和粉砂质组分越多,黏土质组分越少。在泥质细砂岩中,粉砂质次总体与黏土质次总体相关性较弱。

(3) 东河塘组滨岸相沉积物粒度分布可分为细砂质次总体主导型和细砂—极细砂质次总体主导型。细砂质次总体主导型粒度分布中,从细砂岩到泥质细砂岩,黏土质次总体占比逐渐增大、中砂质次

S2次总体最大频率逐渐减小, S6、S7、S8次总体占比逐渐增多

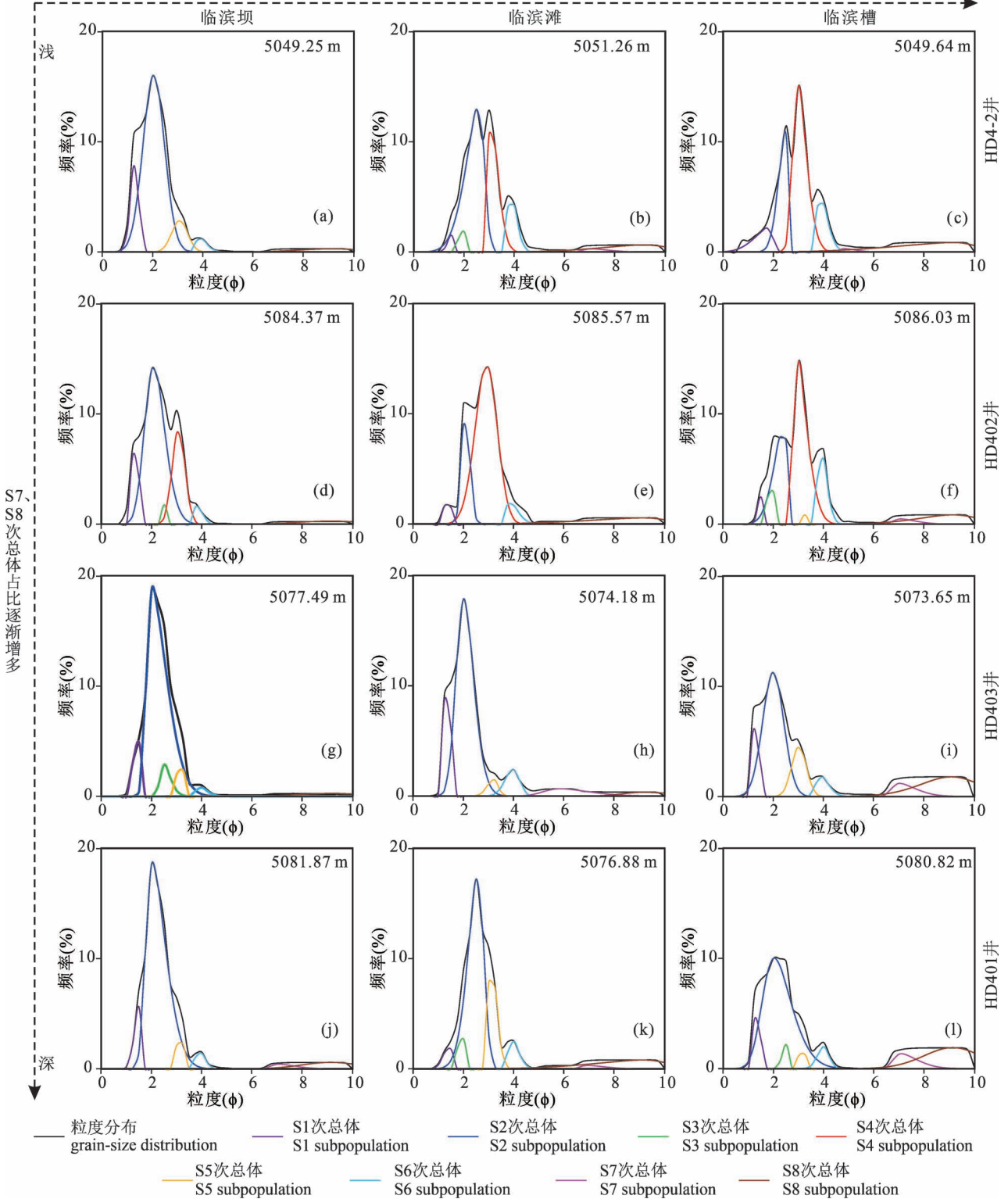


图 11 哈得油田东河塘组横向上不同微相沉积物粒度分布次总体特征

Fig. 11 Subpopulation characteristics of grain-size distributions of horizontal different microfacies sediments from the Donghetang Formation in the Hade Oilfield

总体占比逐渐减小。细砂—极细砂质次总体主导型
粒度分布中,极细砂—粉砂质次总体较发育、中砂质

次总体不发育。

(4) 滨岸相坝体内中砂质次总体占比向上先增

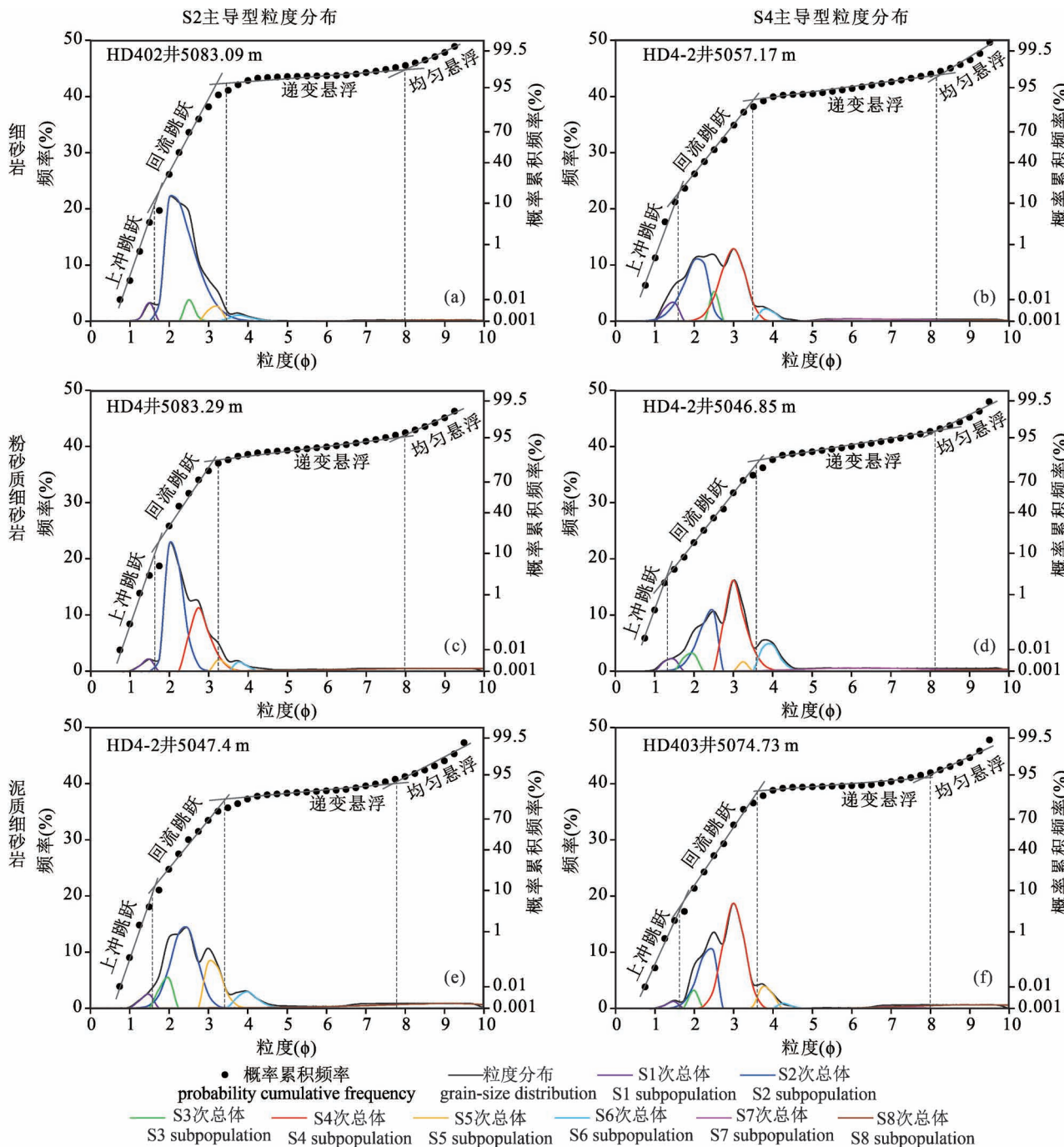


图 12 哈得油田东河塘组滨岸相沉积物不同岩性、不同类型粒度分布概率累计曲线及次总体

Fig. 12 Probability cumulative curves and subpopulations of different lithology and grain-size distribution types of littoral facies sediments from the Donghetang Formation in the Hade Oilfield

大后减小, 指示波浪控制下的沉积动力周期性变化。滩体沉积物中极细砂—粉砂质次总体和粉砂质次总体占比分别大于 8% 和 4%。槽体沉积物中黏土质次总体占比一般大于 6%。向海方向上, 临滨坝、滩、槽内沉积物中主导次总体峰值频率及占比逐渐减小、分选性逐渐变差, 粉砂质次总体与黏土质次总

体逐渐增多。

(5) 滨岸相沉积物粒度分布概率累积曲线为跳跃与悬浮 2 段式, 无滚动组分。跳跃段和悬浮段内又可分别分为 2 部分, 对应上冲跳跃与回流跳跃、递变悬浮与均匀悬浮。中砂质颗粒主要由上冲作用搬运; 细砂质与细砂—极细砂质颗粒主要由回流作用

搬运;极细砂—粉砂质颗粒为跳跃向悬浮搬运的过渡组分;粉砂质与黏土质颗粒分别沉积于递变悬浮和均匀悬浮过程中。

参 考 文 献 / References

(The literature whose publishing year followed by a “&” is in Chinese with English abstract; The literature whose publishing year followed by a “#” is in Chinese without English abstract)

操应长,王健,刘惠民. 2010. 利用环境敏感粒度组分分析滩坝砂体水动力学机制的初步探讨——以东营凹陷西部沙四上滩坝砂体沉积为例. 沉积学报, 28(2): 274~284.

郭兴杰,王寒梅,詹龙喜. 2025. 海岸带地区典型地质灾害链研究进展与展望. 中国工程科学, 27(3): 272~286.

国家能源局. 2009. 碎屑岩粒度分析方法. SY/T 5434—2009.

黄继新,王青春,刘大平,贺萍,惠婧. 2025. 加拿大Dover区块M-W组典型砂质滨岸相沉积演化特征. 河北地质大学学报, 48(4): 37~48.

姜在兴,陈代钊. 2022. 沉积学(3版). 北京:中国石化出版社, 1~608.

姜在兴,王俊辉,张元福. 2015. 滩坝沉积研究进展综述. 古地理学报, 17(4): 427~440.

蒋璟鑫,李超,胡修棉. 2020. 沉积学数据库建设与沉积大数据科学研究进展:以Macrostrat数据库为例. 高校地质学报, 26(1): 27~43.

李维禄,徐怀民,高思宇,江同文,韩如冰,黄素,郭文飞,余义常. 2017. 三角洲改造背景的浪控滨岸砂体成因类型及展布特征——以塔里木盆地东河塘地区“东河砂岩”为例. 中国海洋大学学报(自然科学版), 47(9): 86~95.

林倩闽. 2023. 一种CCA-层次聚类的基因聚类算法. 哈尔滨理工大学学报, 28(5): 85~90.

骆永明. 2016. 中国海岸带可持续发展中的生态环境问题与海岸科学发展. 中国科学院院刊, 31(10): 1133~1142.

马彬彬. 2022. 中强潮海滩沉积变化过程——以北海银滩为例. 导师:戴志军. 上海:华东师范大学博士学位论文.

潘毅,陈自怡,刘焯,朱芳芳,匡翠萍. 2024. 海滩冲流带水沙运动综述. 同济大学学报(自然科学版), 52(6): 920~927.

庞文鸿. 2021. 中强潮海滩沉积动力过程研究——以北海银滩为例. 导师:戴志军. 上海:华东师范大学博士学位论文.

孙东怀,鹿化煜,David Rea,孙有斌,吴胜光. 2000. 中国黄土粒度的双峰分布及其古气候意义. 沉积学报, 18(3): 327~335.

索安宁,曹可,马红伟,王权明,于永海. 2015. 海岸线分类体系探讨. 地理科学, 35(7): 933~937.

王成善,林畅松. 2021. 中国沉积学近十年来的发展现状与趋势. 矿物岩石地球化学通报, 40(6): 1211~1229.

王成善,马永生,彭平安,邹才能,谢树成,肖文交,张水昌,胡修棉,王剑,高抒,侯明才,朱筱敏,邵龙义,吴怀春,刘志飞,陈中强,朱如凯,陈曦. 2025. 从沉积学到沉积圈科学:百年简要回顾与发展展望. 沉积学报, 43(5): 1535~1554.

王萌,牟传龙,梁薇,郑斌嵩,侯乾. 2020. 黔北镇远地区三丘田剖面寒武系明心寺组上段滨岸相沉积特征及其地质意义. 地球科学与环境学报, 42(1): 120~131.

王涛,徐怀民,江同文,陈宣华,刘太勋,方慧京,韩如冰. 2018. 滨岸相砂质输导层非均质性对油气运聚影响研究:以塔里木盆地哈得逊油田东河砂岩为例. 高校地质学报, 24(1): 128~138.

修淳,霍素霞,姚海燕,段海钦,杜明. 2022. 注重新形势下自然岸

线管控的海岸线分类体系探讨. 地理科学, 42(2): 333~342.

叶蓉,邓玄,鲁瑞彬,付晓树,刘娜,何幼斌,李华. 2025. 珠江口盆地滨浅海沉积特征及主控因素. 海洋地质前沿, 41(8): 24~39.

尹力,冯文杰,尹艳树,雷诚,徐庆岩,何一鸣. 2022. 波浪作用下砂质滩坝的沉积过程与沉积模式——基于水槽沉积模拟实验研究. 沉积学报, 40(5): 1393~1405.

余恒,侯晓岚. 2022. 层次聚类算法的天文学应用. 中国科学:物理学 力学 天文学, 52(8): 118~131.

袁瑞,冯文杰,张昌民,赵康,刘家乐,付文俊,王泽宇,孟庆昊,王令辉. 2024. 长江武汉段天兴洲低滩沉积物粒度端元对河流—风成沙丘沉积环境的指示意义. 地质论评, 70(2): 436~448.

袁瑞,张昌民,赵芸,张莉,陈哲,张宝进,黄若鑫. 2022. 基于偏正态概率分布的粒度分布次总体分离及其沉积环境指示意义. 地质论评, 68(3): 1033~1047.

袁瑞. 2025. 大数据背景下粒度分布沉积信息挖掘方法进展. 沉积学报, 43(2): 361~375.

赵俊威,孙海航,张东伟,王恒. 2024. 典型海相砂质临滨坝沉积演化过程及成因机制. 石油与天然气地质, 45(1): 65~80.

赵俊威,王恒,张东伟,孙海航,陈恭洋,印森林. 2025. 海相砂质滩坝沉积构型及表征研究进展. 沉积学报, 43(4): 1275~1292.

赵俊威,徐怀民,江同文,何翠,徐朝晖,阳建平,余义常,王超. 2018. 海平面变化对海相临滨储层微观非均质性的控制作用——以塔里木盆地哈得4油田东河砂岩为例. 中国矿业大学学报, 47(5): 1068~1080.

An Cheng, Parker G, Venditti J G, Lamb M P, Hassan M A, Miwa H, Fu Xudong. 2024. Autogenic formation of bimodal grain size distributions in rivers and its contribution to gravel-sand transitions. Geophysical Research Letters, 51(17): e2024GL109109.

Bergen K J, Johnson P A, de Hoop M V, Beroza G C. 2019. Machine learning for data-driven discovery in solid Earth geoscience. Science, 363(6433): eaa0323.

Blott S J, Pye K. 2012. Particle size scales and classification of sediment types based on particle size distributions: Review and recommended procedures. Sedimentology, 59(7): 2071~2096.

Bright C, Mager S, Horton S. 2020. Response of nephelometric turbidity to hydrodynamic particle size of fine suspended sediment. International Journal of Sediment Research, 35(5): 444~454.

Cao Yingchang, Wang Jian, Liu Huimin. 2010. Preliminary Study on the Hydrodynamic Mechanism of Beach-Bar Sandbodies with Environmentally Sensitive Grain Size Components: A case study from beach-bar sandbody sediments of the upper part of the fourth Member of the Shahejie Formation in the Western Dong. Acta Sedimentologica Sinica, 28(2): 274~284.

Carder K L, Beardsley G F Jr, Pak H. 1971. Particle size distributions in the eastern equatorial Pacific. Journal of Geophysical Research, 76(21): 5070~5077.

Doeglas D J. 1968. Grain-size indices, classification and environment. Sedimentology, 10(2): 83~100.

Folk R L, Ward W C. 1957. Brazos River bar; A study in the significance of grain size parameters. Journal of Sedimentary Research, 27(1): 3~26.

Folk R L. 1954. The distinction between grain size and mineral composition in sedimentary-rock nomenclature. The Journal of Geology, 62(4): 344~359.

Friedman G M. 1961. Distinction between dune, beach, and river sands

- from their textural characteristics. *Journal of Sedimentary Research*, 31(4): 514~529.
- Gan S Q, Scholz C A. 2017. Skew normal distribution deconvolution of grain-size distribution and its application to 530 samples from lake bosumtwi, Ghana. *Journal of Sedimentary Research*, 87(11): 1214~1225.
- Guo Xingjie, Wang Hanmei, Zhan Longxi. 2025&. Typical geological hazard chain in coastal areas: Progress and prospects. *Strategic Study of CAE*, 27(3): 272~286.
- Hartmann D, Flemming B. 2007. From particle size to sediment dynamics: An introduction. *Sedimentary Geology*, 202(3): 333~336.
- Hjulstrom F. 1936. The load of the River Fyris in Central Sweden. *Bulletin Geology Institution University of Upsala*, 25: 221~527.
- Huang Jixin, Wang Qingchun, Liu Daping, He Ping, Hui Jing. 2025&. Sedimentary evolution characteristics of typical sandy shore facies of M-W formation in Dover Block, Canada. *Journal of Hebei GEO University*, 48(4): 37~48.
- Ibbeken H. 1983. Jointed source rock and fluvial gravels controlled by rosin's law: A grain-size study in Calabria, south Italy. *Journal of Sedimentary Research*, 53(4): 1213~1231.
- Jackson N L, Nordstrom K F, Farrell E J. 2017. Longshore sediment transport and foreshore change in the swash zone of an estuarine beach. *Marine Geology*, 386: 88~97.
- James N P, Dalrymple R W. 2010. *Facies models*. Toronto: Geological Association of Canada.
- Jiang Jingxin, Li Chao, Hu Xiumian. 2020&. Advances on sedimentary database building and related research: Macrostrat as an example. *Geological Journal of China Universities*, 26(1): 27~43.
- Jiang Zaixing, Chen Daizhao. 2022#. *Sedimentology (3rd edition)*. Beijing: China Petrochemical Press, 1~608.
- Jiang Zaixing, Wang Junhui, Zhang Yuanfu. 2015&. Advances in beach-bar research: A review. *Journal of Palaeogeography*, 17(4): 427~440.
- Komar P D. 1997. *Beach processes and sedimentation (2nd edition)*. Upper Saddle River: Prentice Hall.
- Kondolf G M, Adhikari A. 2000. Weibull vs. lognormal distributions for fluvial gravels. *Journal of Sedimentary Research*, 70(3): 456~460.
- Krumbein W C, Pettijohn F J. 1938. *Manual of sedimentary petrography*. New York: Appleton-Century-Crofts.
- Li Weilü, Xu Huaimin, Gao Siyu, Jiang Tongwen, Han Rubing, Huang Su, Guo Wenfei, Yu Yichang. 2017&. Genetic types and distribution features of wave-dominated shore deposits with reworked-delta background: A case of 'Donghe sandstones' in donghetang oil field, Tarim Basin. *Periodical of Ocean University of China*, 47(9): 86~95.
- Li Weilü, Xu Huaimin, Yang Jinkun, Gao Siyu, Ning Chaozhong, Yu Yichang, Jiang Tongwen, Wan Fangfang. 2023. Different depositional models of wave-dominated shoreface deposits: An integrated process-oriented analysis ("Donghe sandstones" in Tarim Basin, China). *Marine and Petroleum Geology*, 153: 106288.
- Lin Qianmin. 2023&. A gene clustering algorithm based on the CCA-hierarchical clustering. *Journal of Harbin University of Science and Technology*, 28(5): 85~90.
- Luo Yongming. 2016&. Sustainability associated coastal eco-environmental problems and coastal science development in China. *Bulletin of the Chinese Academy of Sciences*, 31(10): 1133~1142.
- Ma Binbin. 2022&. *Sedimentary change process of medium-strong tidal beach—A case study of Yintan Beach in Beihai City*. Supervisor: Dai Zhijun. Shanghai: East China Normal University Doctoral Dissertation.
- Masselink G, Puleo J A. 2006. Swash-zone morphodynamics. *Continental Shelf Research*, 26(5): 661~680.
- National Energy Administration. 2009#. *Analysis method for particle size of clastic rocks*, SY/T 5434—2009.
- Newton A, Icely J. 2008. Land ocean interactions in the coastal zone, LOICZ: Lessons from banda aceh, Atlantis, and Canute. *Estuarine, Coastal and Shelf Science*, 77(2): 181~184.
- Pan Yi, Chen Ziyi, Liu Ye, Zhu Fangfang, Kuang Cuiping. 2024&. Review on water-sediment movement in swash zone. *Journal of Tongji University (Natural Science)*, 52(6): 920~927.
- Pang Wenhong. 2021&. *Sediment dynamic processes in meso-macro tidal beaches—A case study of Yintan Beach in Beihai City*. Supervisor: Dai Zhijun. Shanghai: East China Normal University Doctoral Dissertation.
- Passessa R. 1964. Grain size representation by CM patterns as a geologic tool. *Journal of Sedimentary Research*, 34(4): 830~847.
- Purkait B. 2002. Patterns of grain-size distribution in some point bars of the Usri river, India. *Journal of Sedimentary Research*, 72(3): 367~375.
- Ramesh R, Chen Z, Cummins V, Day J, D'Elia C, Dennison B, Forbes D L, Glaeser B, Glaser M, Glavovic B, Kremer H, Lange M, Larsen J N, Le Tissier M, Newton A, Pelling M, Purvaja R, Wolanski E. 2015. Land - ocean interactions in the coastal zone: Past, present & future. *Anthropocene*, 12: 85~98.
- Risovic D. 1993. Two-component model of sea particle size distribution. *Deep Sea Research Part I: Oceanographic Research Papers*, 40(7): 1459~1473.
- Román-Sánchez A, Temme A, Willgoose G, van den Berg D, Gura C M, Vanwallegem T. 2021. The fingerprints of weathering: Grain size distribution changes along weathering sequences in different lithologies. *Geoderma*, 383: 114753.
- Sahu B K. 1964. Depositional mechanisms from the size analysis of clastic sediments. *Journal of Sedimentary Research*, 34(1): 73~83.
- shley G M. 1978. Interpretation of polymodal sediments. *The Journal of Geology*, 86(4): 411~421.
- Sternberg H. 1875. Untersuchungen uber langend querprofil geschiebefuhrender flusse. *Zeitschrift fur Bauwesen*, 25: 483~506.
- Sun Donghuai, Bloemendal J, Rea D K, An Zhisheng, Vandenberghe J, Lu Huayu, Su Ruixia, Liu T. 2004. Bimodal grain-size distribution of Chinese loess, and its palaeoclimatic implications. *Catena*, 55(3): 325~340.
- Sun Donghuai, Bloemendal J, Rea D K, Vandenberghe J, Jiang Fuchu, An Zhisheng, Su Ruixia. 2002. Grain-size distribution function of polymodal sediments in hydraulic and aeolian environments, and numerical partitioning of the sedimentary components. *Sedimentary Geology*, 152(3~4): 263~277.
- Sun Donghuai, Lu Huayu, Rea David, Sun Youbin, Wu Shengguang. 2000&. Bimode grain-size distribution of Chinese loess and its paleoclimate implication. *Acta Sedimentologica Sinica*, 18(3): 327~335.
- Suo Anning, Cao Ke, Ma Hongwei, Wang Quanming, Yu Yonghai. 2015&. Discussion on classification system of coastline. *Scientia*

- Geographica Sinica, 35(7): 933~937.
- Udden J A. 1898. The mechanical composition of wind deposits. Illinois: Augustana Library Publications, 3(1): 1~69.
- Udden J A. 1914. Mechanical composition of clastic sediments. Geological Society of America Bulletin, 25(1): 655~744.
- van Hateren J A, Prins M A, van Balen R T. 2018. On the genetically meaningful decomposition of grain-size distributions: A comparison of different end-member modelling algorithms. Sedimentary Geology, 375: 49~71.
- Visher G S. 1969. Grain size distributions and depositional processes. Journal of Sedimentary Research, 39(3): 1074~1106.
- Wang Chengshan, Lin Changsong. 2021&. Development status and trend of sedimentology in China in recent ten years. Bulletin of Mineralogy, Petrology and Geochemistry, 40(6): 1211~1229.
- Wang Chengshan, Ma Yongsheng, Peng Ping'an, Zou Caineng, Xie Shucheng, Xiao Wenjiao, Zhang Shuichang, Hu Xiumian, Wang Jian, Gao Shu, Hou Mingcai, Zhu Xiaomin, Shao Longyi, Wu Huaichun, Liu Zhifei, Chen Zhongqiang, Zhu Rukai, Chen Xi. 2025&. A century journey from sedimentology to sedimentosphere science: Review and perspective. Acta Sedimentologica Sinica, 43(5): 1535~1554.
- Wang Meng, Mou Chuanlong, Liang Wei, Zheng Binsong, Hou Qian. 2020&. Sedimentary characteristics of the shore facies of Cambrian upper mingxinsi formation in Sanqiutian profile of Zhenyuan area, the northern Guizhou, China and their geological significance. Journal of Earth Sciences and Environment, 42(1): 120~131.
- Wang Tao, Xu Huaimin, Jiang Tongwen, Chen Xuanhua, Liu Taixun, Fang Huijing, Han Rubing. 2018&. Influence of heterogeneity of sandy carrier bed of littoral facies on hydrocarbon migration and accumulation: A case of the Donghe sandstone in the hadexun area, Tarim Basin, China. Geological Journal of China Universities, 24(1): 128~138.
- Weltje G J, Prins M A. 2007. Genetically meaningful decomposition of grain-size distributions. Sedimentary Geology, 202(3): 409~424.
- Wentworth C K. 1922. A scale of grade and class terms for clastic sediments. The Journal of Geology, 30(5): 377~392.
- Wu Li, Krijgsman W, Liu Jian, Li Chaozhu, Wang Rujian, Xiao Wenshen. 2020. CFLab: A MATLAB GUI program for decomposing sediment grain size distribution using Weibull functions. Sedimentary Geology, 398: 105590.
- Xiao Jule, Chang Zhigang, Fan Jiawei, Zhou Lang, Zhai Dayou, Wen Ruilin, Qin Xiaoguang. 2012. The link between grain-size components and depositional processes in a modern clastic lake. Sedimentology, 59(3): 1050~1062.
- Xiu Chun, Huo Suxia, Yao Haiyan, Duan Haiqin, Du Ming. 2022&. Coastline classification for strictly controlling natural coastline in the new era. Scientia Geographica Sinica, 42(2): 333~342.
- Ye Rong, Deng Xuan, Lu Ruibin, Fu Xiaoshu, Liu Na, He Youbin, Li Hua. 2025&. Sedimentary characteristics and main controlling factors of coastal shallow sea deposits in the Pearl River Mouth Basin. Marine Geology Frontiers, 41(8): 24~39.
- Yin Li, Feng Wenjie, Yin Yanshu, Lei Cheng, Xu Qingyan, He Yiming. 2022&. Process and Model of Sedimentation of Sandy Beach Bar Due to Wave Action: An experimental study based on sink sedimentation simulation. Acta Sedimentologica Sinica, 40(5): 1393~1405.
- Yu Heng, Hou Xiaolan. 2022. Hierarchical clustering in astronomy. Scientia Sinica (Physica, Mechanica & Astronomica), 52(8): 118~131.
- Yuan Rui, Feng Wenjie, Zhang Changmin, Zhao Kang, Liu Jiale, Fu Wenjun, Wang Zeyu, Meng Qinghao, Wang Linghui. 2024&. Fluvial—aeolian dune depositional environment significances from grain-size end-member in low-beach at the head of Tianxing Central-bar in Wuhan section of Yangtze River. Geological Review, 70(2): 436~448.
- Yuan Rui, Yan Zijin, Zhu Rui, Wang Chao, Yuan Rui, Yan Zijin, Zhu Rui, Wang Chao. 2025a. Multifractal characteristics of grain size distributions in braided delta-front: A case of Paleogene Enping Formation in huilu low uplift, Pearl River mouth basin, South China Sea. Fractal and Fractional, 9(4): 216.
- Yuan Rui, Lu Chenlong, Zhao An, Wang Wei, Wu Zhiwei, Yan Zijin, Sun Qi. 2025b. Quantitative recognition and petroleum geological significance of interlayers in coastal sandstone reservoirs: A case study from the Donghe Sandstone in the Hade Oilfield, Tarim Basin, NW China. Energy Geoscience, 6(4): 100439.
- Yuan Rui, Zhang Changmin, Zhao Yun, Zhang Li, Chen Zhe, Zhang Baojin, Huang Ruoxin. 2022&. Decomposing subpopulations from grain-size distributions based on skew normal probability distribution and their significances for sedimentary environments. Geological Review, 68(3): 1033~1047.
- Yuan Rui. 2025&. Progress on mining methods of sedimentological information from grain-size distribution under the background of big data. Acta Sedimentologica Sinica, 43(2): 361~375.
- Zhao Jier, Fan Yiren, Ge Xinmin, Wang Wei, Zhu Zhengjun, Wang Min, Zhao Dongyue. 2023. An intelligent identification method of interlayers in deep clastic rock - An example of Donghe Sandstone in Hade Oilfield, Tarim Basin. Marine and Petroleum Geology, 156: 106419.
- Zhao Junwei, Sun Haihang, Zhang Dongwei, Wang Heng. 2024&. Sedimentary evolution and genetic mechanisms of typical marine nearshore sandbars. Oil & Gas Geology, 45(1): 65~80.
- Zhao Junwei, Wang Heng, Zhang Dongwei, Sun Haihang, Chen Gongyang, Yin Senlin. 2025&. Advances in sedimentary architecture and characterization of marine sandy beach-bars: A review. Acta Sedimentologica Sinica, 43(4): 1275~1292.
- Zhao Junwei, Xu Huaimin, He Cui, Jiang Tongwen, Xu Zhaohui, Yang Jianping, Wang Chao, Yu Yichang. 2017. Control mechanism of sea level rise and fall on the macroscopic heterogeneity of marine reservoirs: An example of the Donghe sandstone reservoir in the hadeson oilfield, Tarim Basin. Geology and Exploration, 53(3): 590~598.
- Zhao Junwei, Xu Huaimin, Jiang Tongwen, He Cui, Xu Zhaohui, Yang Jianping, Yu Yichang, Wang Chao. 2018&. The controlling effect of sea level changing on the microscopic heterogeneity of marine reservoir: Taking shoreface subfacies reservoir of Donghe sandstone in Hade 4 oilfield as an example. Journal of China University of Mining & Technology, 47(5): 1068~1080.

Sedimentary significances mining from subpopulations in grain-size distributions of littoral facies sediments:

A case study of the Donghetang Formation in the Hade Oilfield, Tarim Basin

YUAN Rui¹⁾, LIU Xue¹⁾, ZHU Rui²⁾, HAN Denglin²⁾

1) *School of Geophysics and Petroleum Resources, Yangtze University, Wuhan, 430100;*

2) *School of Geosciences, Yangtze University, Wuhan, 430100*

Objective: Littoral facies is a kind of transitional environment between marine and terrestrial deposition. Controlled by complex sedimentary dynamic mechanisms, frequency curves of grain-size distributions of littoral facies sediments are usually multimodal. The subpopulations of grain-size distributions are the recorders of original depositional information contained in littoral facies. In order to mine sedimentary significances from subpopulations in grain-size distributions of littoral facies sediments, ancient littoral sand body in the Donghetang Formation in the Hade Oilfield, Tarim Basin, was investigated in this paper.

Methods: Skew normal probability density function is used to decompose 968 subpopulations from 156 grain-size distributions. These subpopulations are automatically classified by hierarchical clustering. Relevance, combination mode, depositional environment significances and transport way of subpopulations are discussed in Pearson correlation coefficient, microfacies and probability cumulative curves.

Results: In this paper, the results show that all subpopulations can be classified into 8 types. With the increment of fine sandy dominant subpopulations' percentages in grain-size distributions, medium sandy subpopulations' proportions increase and fine-very fine sandy subpopulations' proportions reduce. Medium sandy subpopulations' proportions firstly increase and then decrease from bottom to top in bar sands. Proportions of fine-very fine sandy and silty subpopulations are markedly increased in beach sands. Proportions of clay subpopulations are over 6% in trough sands. From bar to beach and trough in shoreface seaward, peak frequencies of fine sandy dominant subpopulations decrease and sorting are worse, and silty and clay subpopulations increase gradually. Medium sandy particles were transported by swash, while fine and very fine sandy grains were transported by backwash mainly. Silty and clay grains deposited in graded and uniform suspension respectively.

Conclusions: Depositional information mined from subpopulations of grain-size distributions offers references for researching sedimentary environments and evolutionary processes of modern and ancient littoral facies sediments.

Keywords: Tarim Basin; Donghetang Formation; littoral facies; sediments; grain-size distribution; subpopulation

Acknowledgements: This research is supported by Natural Science Foundation of China (No. 42202113)

First author: YUAN Rui, male, born in 1987, doctor, associate professor, master supervisor, is mainly engaged in research and teaching of data mining of geoscience and logging geology; Email: yuanrui@yangtzeu.edu.cn

Manuscript received on: 2025-11-10; Accepted on: 2026-01-19; Published online on: 2026-02-15

Doi: 10.16509/j.georeview.2026.02.011

Edited by: LIU Zhiqiang